

Improving Network Robustness against Adversarial Attacks with Compact Convolution

Rajeev Ranjan, Swami Sankaranarayanan, Carlos D. Castillo and Rama Chellappa
 Center for Automation Research, UMIACS, University of Maryland, College Park, MD 20742
 {rjan1,swamiviv,carlos,rama}@umiacs.umd.edu

Abstract

Though Convolutional Neural Networks (CNNs) have surpassed human-level performance on tasks such as object classification and face verification, they can easily be fooled by adversarial attacks. These attacks add a small perturbation to the input image that causes the network to mis-classify the sample. In this paper, we focus on neutralizing adversarial attacks by exploring the effect of different loss functions such as CenterLoss and L2-Softmax Loss for enhanced robustness to adversarial perturbations. Additionally, we propose power convolution, a novel method of convolution that when incorporated in conventional CNNs improve their robustness. Power convolution ensures that features at every layer are bounded and close to each other. Extensive experiments show that Power Convolutional Networks (PCNs) neutralize multiple types of attacks, and perform better than existing methods for defending adversarial attacks.

1. Introduction

In recent years, CNNs have gained tremendous popularity because of their impressive performance on many vision-related tasks. They are being widely used in many practical applications such as self-driving cars, face verification, etc. However, it has been shown that CNNs are vulnerable to even small adversarial perturbations which, when added to the input image, can cause the network to mis-classify with high confidence [26, 6, 18, 17]. Adversarial images thus generated are often visually indistinguishable from the original images.

Adversarial attacks have emerged as a potential threat to the CNN-based systems. Adversarial images can be used by a suspect to fool a face verification system, by letting the person go unidentified. They can be used by a hacker to surpass a face authentication system and gain unauthorized access. These attacks can also cause self-driving cars to mis-classify scene objects such as a stop sign leading to adverse effects when these systems are deployed in real time.

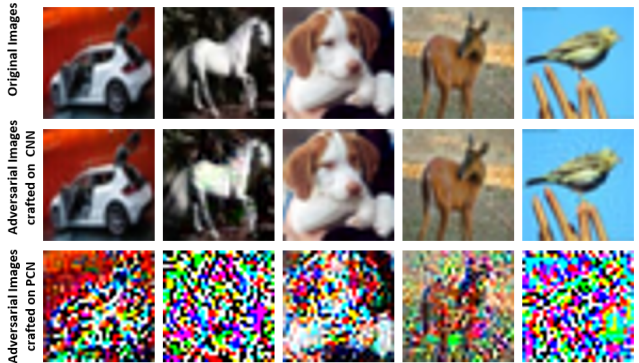


Figure 1. Five test samples from CIFAR10 [10] dataset (top) that are correctly classified by both CNN and PCN. Corresponding adversarial images crafted using DeepFool [18] attack and misclassified by CNN (middle) and PCN (bottom). The adversarial attacks on PCN can be detected trivially by human observer.

Due to these vulnerabilities in CNN, it is crucial to design networks that are not only accurate, but also robust to adversarial perturbations. We propose to improve network's robustness by analyzing key properties required for defending against adversarial attacks.

It has been hypothesized that CNNs learn a highly non-linear manifold on which the images of same class lie together, while images from different class are separated. Hence, the original image and the adversarial image lying close to each other in Euclidean space, are far separated on the manifold or in feature space. When designing a robust classifier, we would like to address the following question: *Does bringing the original and perturbed image closer in the feature space of a learned mapping improve its robustness?* To address this question, we postulate two important properties that would enhance a network's robustness to adversarial attacks: 1) *Centrality* and 2) *Compactness*. *Centrality* adds an additional constraint that features of same class should lie very close to each other in Euclidean space. This constraint enforces the features of the perturbed image to lie closer to the class center and far from the classifier boundary, thus improving its robustness. *Compactness* enforces the features to be bounded and lie in a closed space.

It restricts the extent to which a feature for perturbed image can move, making it less likely to cross the class boundary.

To enforce *centrality* and *compactness* constraints to the network features, we explore different loss functions such as CenterLoss [28] and L_2 -Softmax Loss [22]. The CenterLoss establishes *centrality* by penalizing the distance between the features from the last layer of the network and their corresponding class centers. L_2 -Softmax Loss establishes both *compactness* and *centrality* by constraining the features to lie on a hypersphere of fixed radius, before applying the softmax loss. We show that the robustness of CNNs to adversarial attacks can be improved by training the network with these loss functions.

Using these insights, we propose a novel convolution method, called *power convolution*, that significantly enhances a network’s robustness by enforcing layer-wise *centrality* and *compactness*. A power convolution module applies L_2 -normalization and scaling operations to every input patch before applying the convolutional kernel in a sliding window fashion. Power Convolutional Networks (PCNs), built using these modules, are highly robust compared to a typical CNN. Figure 1 shows some sample images and corresponding adversarial attacks generated using DeepFool [18] to fool a CNN and a PCN. The adversarial samples for PCN can easily be distinguished from the original samples by a human observer. The paper makes the following key contributions:

- We explore two important properties of the features learned by a network, namely *Centrality* and *Compactness*, and show their necessity in making a network robust to adversarial attacks.
- We propose to use CenterLoss and L_2 -Softmax Loss as defense mechanisms against adversarial perturbations.
- We propose power convolutional modules that increases the network stability by applying the *Centrality* and *Compactness* properties to features at every layer in the network.
- We achieve new state-of-the-art results on defending white-box as well as black-box attacks.

2. Related Works

A lot of research has gone into generating adversarial perturbations to fool a deep network. Szegedy et al. [26] first showed the existence of adversarial perturbations in CNNs and proposed a L-BFGS based optimization scheme to generate the same. Later, Goodfellow et al. [6] proposed Fast Gradient Sign Method (FGSM) to generate adversarial samples. DeepFool [18] attack iteratively finds a minimal perturbation required to cause a network to mis-classify. Other recently proposed adversarial attacks include Jacobian-based Saliency Map Approach (JSMA) [20], Carlini-Wagner (CW) attack [2], Universal Perturbations [17], etc.

To safeguard the network from adversarial attacks, re-

searchers have focused on two approaches: 1) *Adversarial Detection*, and 2) *Adversarial Defense*. Methods based on adversarial detection [14, 15, 7, 5] attempt to detect an adversarial sample before passing it through the network for inference. These methods put an extra effort in designing a separate adversarial detector which itself has the risk of being fooled by the attacker. Recently, Carlini and Wagner [1] showed that most of the adversarial detectors are ineffective and can be bypassed.

The methods based on adversarial defense aim at improving the network’s robustness to classify adversarial samples correctly. One way to achieve robustness is by simultaneously training the network with clean and adversarial samples [6, 16, 24, 11]. These methods are stable to the attack on which they are trained, but ineffective against a different attack. Preprocessing the input to nullify the adversarial effect is another way to defend the network [4, 9]. Few methods have focused on modifying the network topology or optimization procedure for adversarial defense. Gu and Rigazio [8] proposed Deep Contractive Network that adds a smoothness penalty on the partial derivatives at every layer. Cisse et al. [3] proposed Parseval Networks that improves robustness by enforcing the weight matrices of convolutional and linear layers to be Parseval tight frames. Papernot et al. [21] showed that knowledge distillation with high temperature parameter can be used as defense against adversarial samples. Warde et al. [27] showed that a similar robustness as defensive distillation can be obtained by training the network with smooth labels. Zantedeschi et al. [29] used Bounded ReLU activations to enhance network’s stable to adversarial perturbations.

While these methods have focused on improving defense to adversarial attacks in general, most of them have focused on white box attacks and incur additional computational overhead during training. In this work, we propose an approach to achieve adversarial defense in CNN using power convolutions which can be seamlessly integrated into any existing deep network architecture. We further demonstrate its effectiveness against both white box and black box adversarial attacks.

3. Adversarial Defense

In this section, we prove the necessity of *centrality* and *compactness* of the network features for improved robustness to adversarial attacks. Let \mathbf{x} be the input image. Let $\tilde{\mathbf{x}}$ and $\tilde{\mathbf{x}}_r$ be the corresponding feature vectors from networks \hat{k} and \hat{k}_r respectively. Both these networks have same architecture and number of parameters. Let the classification score for a feature \mathbf{t} be given by: $f(\mathbf{t}) = \mathbf{W}^T \mathbf{t} + b$. For an input perturbation η , the corresponding perturbations in feature space are $\tilde{\eta}$ and $\tilde{\eta}_r$ for networks \hat{k} and \hat{k}_r respectively. From [18] we know that the direction of a typical adversarial perturbation in feature space is opposite to the

classifier weight vector W . The perturbations $\tilde{\eta}$ and $\tilde{\eta}_r$ can be rewritten as:

$$\tilde{\eta} = -\gamma \hat{W}, \quad \tilde{\eta}_r = -\gamma_r \hat{W}, \quad (1)$$

where γ and γ_r are the magnitudes of the perturbations $\tilde{\eta}$ and $\tilde{\eta}_r$ obtained from the respective networks, \hat{W} is the unit-vector of the classifier weight. Let \mathbb{E}_x denote the expectation operator over the input data. We say that the network \hat{k}_r is more robust than \hat{k} if the expected classification score for the adversarial inputs is higher with \hat{k}_r , i.e.,

$$\mathbb{E}_x[W^T(\tilde{\mathbf{x}}_r + \tilde{\eta}_r) + b] > \mathbb{E}_x[W^T(\tilde{\mathbf{x}} + \tilde{\eta}) + b]. \quad (2)$$

Since the networks \hat{k} and \hat{k}_r have similar architecture and performance accuracy, it is reasonable to assume that the expected classification scores for the unperturbed inputs is same for both of them:

$$\mathbb{E}_x[W^T \tilde{\mathbf{x}}_r + b] = \mathbb{E}_x[W^T \tilde{\mathbf{x}} + b]. \quad (3)$$

Using (3), (2) reduces to:

$$\mathbb{E}_x[W^T \tilde{\eta}_r] > \mathbb{E}_x[W^T \tilde{\eta}]. \quad (4)$$

Using (1), we can rewrite (4) as:

$$\mathbb{E}_x[W^T(-\gamma_r \hat{W})] > \mathbb{E}_x[W^T(-\gamma \hat{W})] \quad (5)$$

$$\mathbb{E}_x[\gamma_r] < \mathbb{E}_x[\gamma] \quad (6)$$

(6) implies that a network \hat{k}_r is more robust or harder to be fooled than network \hat{k} if the magnitude of the generated perturbation in the feature space is smaller for \hat{k}_r compared to \hat{k} . Using the above equations, we justify the *centrality* and *compactness* properties in the following propositions.

Proposition 1 (Centrality): Let $\tilde{\mu}$ and $\tilde{\mu}_r$ be the class centers in feature space for the networks \hat{k} and \hat{k}_r respectively. \hat{k}_r is more robust than \hat{k} if:

$$\mathbb{E}_x[\|\tilde{\mathbf{x}}_r - \tilde{\mu}_r\|_2^2] < \mathbb{E}_x[\|\tilde{\mathbf{x}} - \tilde{\mu}\|_2^2] \quad (7)$$

Proof: Using condition (7), we need to show that (6) holds. Expanding (7), we get:

$$\begin{aligned} \mathbb{E}_x[\|\tilde{\mathbf{x}}_r\|_2^2] - 2\mathbb{E}_x[\tilde{\mathbf{x}}_r^T \tilde{\mu}_r] + \mathbb{E}_x[\|\tilde{\mu}_r\|_2^2] &< \\ \mathbb{E}_x[\|\tilde{\mathbf{x}}\|_2^2] - 2\mathbb{E}_x[\tilde{\mathbf{x}}^T \tilde{\mu}] + \mathbb{E}_x[\|\tilde{\mu}\|_2^2] \end{aligned} \quad (8)$$

Using 7,

$$\mathbb{E}_x[\|\tilde{\mathbf{x}}_r + \tilde{\eta}_r - \tilde{\mu}_r\|_2^2] < \mathbb{E}_x[\|\tilde{\mathbf{x}} + \tilde{\eta} - \tilde{\mu}\|_2^2] \quad (9)$$

Expanding (9), we get:

$$\begin{aligned} \mathbb{E}_x[\|\tilde{\mathbf{x}}_r + \tilde{\eta}_r\|_2^2] - 2\mathbb{E}_x[(\tilde{\mathbf{x}}_r + \tilde{\eta}_r)^T \tilde{\mu}_r] + \mathbb{E}_x[\|\tilde{\mu}_r\|_2^2] &< \\ \mathbb{E}_x[\|\tilde{\mathbf{x}} + \tilde{\eta}\|_2^2] - 2\mathbb{E}_x[(\tilde{\mathbf{x}} + \tilde{\eta})^T \tilde{\mu}] + \mathbb{E}_x[\|\tilde{\mu}\|_2^2] \end{aligned} \quad (10)$$

Subtracting (8) from (10), we obtain:

$$\begin{aligned} \mathbb{E}_x[\|\tilde{\eta}_r\|_2^2] + 2\mathbb{E}_x[\tilde{\eta}_r^T (\tilde{\mathbf{x}}_r - \tilde{\mu}_r)] &< \\ \mathbb{E}_x[\|\tilde{\eta}\|_2^2] + 2\mathbb{E}_x[\tilde{\eta}^T (\tilde{\mathbf{x}} - \tilde{\mu})] \end{aligned} \quad (11)$$

Since $\mathbb{E}_x[\tilde{\mathbf{x}} - \tilde{\mu}] = \mathbb{E}_x[\tilde{\mathbf{x}}_r - \tilde{\mu}_r] = 0$, using linearity of expectation operator the second term from both L.H.S and R.H.S of (11) gets eliminated and we get:

$$\mathbb{E}_x[\|\tilde{\eta}_r\|_2^2] < \mathbb{E}_x[\|\tilde{\eta}\|_2^2] \quad (12)$$

Substituting the perturbations from (1) in (12), we get

$$\mathbb{E}_x[\|\gamma_r\|_2^2] < \mathbb{E}_x[\|\gamma\|_2^2], \quad (13)$$

which is equivalent to (6). This shows that *centrality* improves robustness against adversarial attacks.

Proposition 2 (Compactness): Let M be a fixed constant. \hat{k}_r is more robust than \hat{k} if $\tilde{\mathbf{x}}_r$ lies inside a p -norm ball:

$$\|\tilde{\mathbf{x}}_r\|_p \leq M, \quad p \geq 1 \quad (14)$$

Proof: Using (14) for the adversarial samples, we get:

$$\|\tilde{\mathbf{x}}_r + \tilde{\eta}_r\|_p \leq M \quad (15)$$

(15) implies that the adversarial perturbation will be clipped if the p -norm of the perturbed feature exceeds a constant. The bounded perturbation $\tilde{\eta}_r$ can be written in terms of unbounded perturbation $\tilde{\eta}$ as:

$$\tilde{\eta}_r = \begin{cases} \tilde{\eta} & \text{if } \|\tilde{\mathbf{x}}_r + \tilde{\eta}\|_p \leq M \\ \tilde{\eta}_c \text{ s.t. } \|\tilde{\mathbf{x}}_r + \tilde{\eta}_c\|_p = M & \text{if } \|\tilde{\mathbf{x}}_r + \tilde{\eta}\|_p > M \end{cases} \quad (16)$$

Using equivalence of norms, (16) implies that:

$$\|\tilde{\eta}_r\|_2 \leq \|\tilde{\eta}\|_2 \quad (17)$$

Substituting the perturbations from (1) in (17), we obtain (6) which proves that *compactness* makes a network more robust to adversarial attacks.

4. Robust Loss Functions

In this section, we provide an overview of CenterLoss [28] and L_2 -Softmax Loss [22], which enhance the network's robustness to adversarial attacks by following the principles of *centrality* and *compactness*.

4.1. CenterLoss

The CenterLoss was proposed by Wen et al. [28] for the task of discriminative face verification. It simultaneously learns a center for deep features of each class and penalizes the distances between the deep features and their corresponding class centers. The structure of the loss function is shown in (18):

$$L_C = -\sum_{i=1}^m \log \frac{e^{W_{y_i}^T \mathbf{x}_i + b_{y_i}}}{\sum_{j=1}^n e^{W_j^T \mathbf{x}_i + b_j}} + \lambda \frac{1}{2} \sum_{i=1}^m \|\mathbf{x}_i - \mathbf{c}_{y_i}\|_2^2, \quad (18)$$

where \mathbf{x}_i is the i^{th} deep feature and \mathbf{c}_{y_i} is the center for the class label y_i , W_j is the weight and b_j is the bias

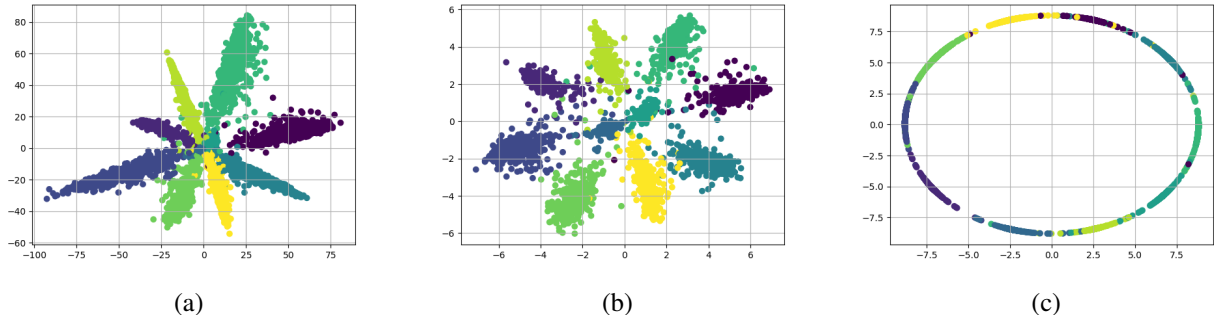


Figure 2. Feature visualization from the last layer (dimension=2) of CNN trained on MNIST [13] with (a) Softmax Loss, (b) Center Loss and (c) L_2 -Softmax Loss.

corresponding to the class j , and m, n are the batch-size and number of classes respectively. The first term is the typical softmax loss that encourages inter-class separability. The second term is the distance penalty that ensures the closeness of intra-class deep features. The hyper-parameter λ controls the trade-off between intra-class and inter-class variability.

We use CenterLoss as a defense to adversarial attacks owing to its *centrality* property. Experimental results suggest that CenterLoss improves network robustness compared to traditional softmax loss.

4.2. L_2 -Softmax Loss

L_2 -Softmax loss was recently proposed by Ranjan et al. [22] for improving the task of face verification. The loss imposes a constraint on the deep features to lie on a hypersphere of a fixed radius, before applying the softmax penalty. The loss is defined as:

$$L_S = - \sum_{i=1}^m \log \frac{e^{W_{y_i}^T (\frac{\alpha \mathbf{x}_i}{\|\mathbf{x}_i\|_2}) + b_{y_i}}}{\sum_{j=1}^n e^{W_j^T (\frac{\alpha \mathbf{x}_i}{\|\mathbf{x}_i\|_2}) + b_j}}, \quad (19)$$

where \mathbf{x}_i is the i^{th} deep feature for the class label y_i , W_j is the weight and b_j is the bias corresponding to the class j , α is a positive scalar parameter, and m, n are the batch-size and number of classes respectively. The features are first normalized to unit length and then scaled by α before passing it through the softmax classifier. Constraining the features to lie on a hypersphere reduces the intra-class variations and enhances the inter-class separability.

Unlike CenterLoss, the L_2 -Softmax Loss possesses both *centrality* and *compactness* properties. The *compactness* comes from the fact that the L_2 -norm of the feature vector is always constant and equal to α . The *centrality* is inherently implied since the softmax loss enforces the feature vectors of class j to lie closer to the point $\alpha \hat{W}_j$ on the hypersphere, where \hat{W}_j denotes the unit weight vector for the j^{th} class.

From Figure 2, we can see that the features trained using softmax loss do not satisfy the *centrality* and *compactness*

properties. The CenterLoss enforces *centrality*, while L_2 -Softmax Loss enforces both *centrality* and *compactness* on the CNN features. Experimental analysis (see section 6) shows that both CenterLoss and L_2 -Softmax Loss are more robust to adversarial attacks than softmax loss.

5. Power Convolution

The L_2 -Softmax loss applies the *centrality* and *compactness* properties only to the deep features from the last layer of CNN. We propose to extend these properties to features from the intermediate layers of CNNs as well. A typical CNN is a hierarchy of convolutional and fully-connected layers stacked with non-linear activation functions after every layer. A discrete convolution is a linear function applied on a patch of a signal in a sliding window fashion. Let W be the convolution kernel of size $2k + 1$, $\mathbf{x}_{n,k}$ be an input patch defined as:

$$\mathbf{x}_{n,k} = [x(n-k), x(n-k+1), \dots, x(n+k)], \quad (20)$$

where $x(n)$ is the n^{th} element of input vector \mathbf{x} . The convolution operation is represented as:

$$y(n) = W^T \mathbf{x}_{n,k}, \quad (21)$$

where $y(n)$ is the n^{th} element of the output vector \mathbf{y} . To enforce *centrality* and *compactness* in convolutional layers, we need to ensure that every input patch at a given location is first L_2 -normalized and scaled before multiplying with the convolutional kernel W . Formally, we want the convolution output ($\tilde{y}(n)$) at position n to be:

$$\tilde{y}(n) = W^T \frac{(\alpha \mathbf{x}_{n,k})}{\|\mathbf{x}_{n,k}\|_2 + \delta}, \quad (22)$$

where δ is a small constant added to avoid division by zero. We call this new method of patch-normalized convolution as *power convolution*. A toy example depicting the difference between typical convolution and power convolution is shown in Figure 3.

In a deep CNN, the convolution kernel is typically applied to high dimensional feature maps. Normalizing every feature patch before multiplying with the convolutional

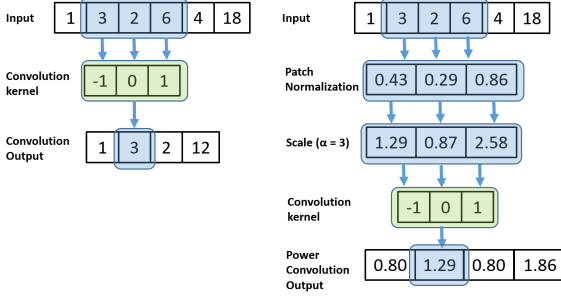


Figure 3. A toy example for convolution (left) and power convolution (right).

kernel is computationally expensive and redundant, since the patches are overlapping. To implement power convolution efficiently in a deep network, we propose a power convolution module (shown in Figure 4). We split the input feature map into two branches. The first branch carries out the traditional convolution operation with parameters of size $k \times k$, without bias addition. The second branch first computes the sum of squares along the channel dimension of the input. Subsequently, it is convolved with a $k \times k$ kernel containing fixed value of all ones. This step provides the squared L_2 -Norm of sliding-window patches for every output location in a feature map. We perform element-wise square-root on top of it and add a small constant $\delta = 0.01$. Lastly, the convolutional output from the first branch is divided element-wise with the output from the second branch. We then scale the final output with a learnable scalar parameter α and add the bias term. The power convolution module uses just one extra parameter (α) compared to the traditional convolutional layer.

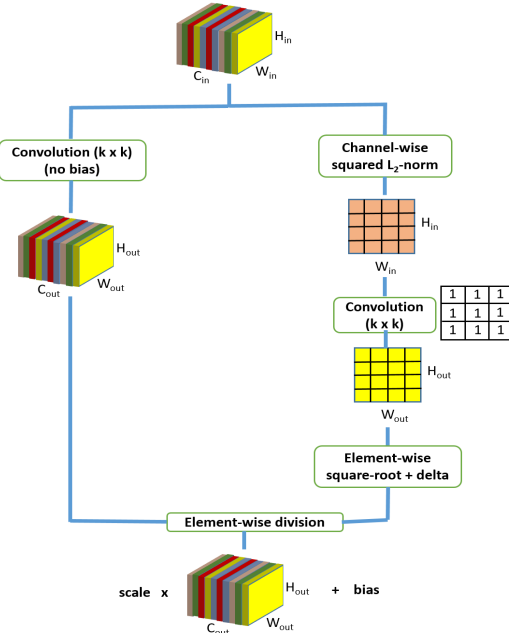


Figure 4. Block diagram of a power convolution module.

Since the linear operation in fully-connected layers is a special case of convolution, the power convolution operation for these layers results in L_2 -normalization and scaling of the feature vectors. It constrains the features to lie on a hypersphere of fixed radius (α), before applying the dot product with the layer parameters. Deep networks with power convolution modules are termed as Power Convolutional Networks (PCNs). They follow the *centrality* and *compactness* property at every layer of the network, which greatly enhances their robustness against multiple kinds of adversarial attacks. The L_2 -Softmax Loss inherently gets applied in PCNs.

6. Experiments

We evaluate the effectiveness of the proposed defense methods on MNIST [13] and CIFAR10 [10] datasets. MNIST [13] dataset contains 60,000 training and 10,000 test images of handwritten digits. The images are 28×28 dimensional with values in $[0, 1]$. CIFAR10 [10] dataset contains 50,000 training and 10,000 test images of 10 classes. The images are $32 \times 32 \times 3$ dimensional, with values scaled between 0 and 1.

We use two well-known methods for crafting adversarial attacks: Fast Gradient Sign Method [6] (FGSM) and DeepFool [18]. FGSM attack adds the sign of the gradient to the input, scaled by the factor ϵ as shown in equation 23

$$\tilde{\mathbf{x}} = \mathbf{x} + \epsilon \text{sign}(\nabla_{\mathbf{x}} J(\theta, \mathbf{x}, y)), \quad (23)$$

where \mathbf{x} is the input image, $\tilde{\mathbf{x}}$ is the crafted adversarial image, $\nabla_{\mathbf{x}} J(\theta, \mathbf{x}, y)$ is gradient of the cost function with respect to the input. This method is very fast, since it uses a single backward step to generate the attack. On the other hand, DeepFool [18] iteratively finds the minimal perturbation required to mis-classify the input in the direction of the nearest class boundary. Though being slower than FGSM [6], DeepFool [18] can generate adversarial images with smaller magnitude of perturbations, which are indistinguishable to human observer. We use the Foolbox [23] library to generate these attacks. We also provide experimental analysis using other adversarial attacks in the supplementary.

The network architectures used for training are provided in Table 1. For training on MNIST [13], we use the architecture proposed by Papernot et al. [21]. The learning rate is set to 0.1 for the first thirty epochs, and decreased by a factor of 0.1 after every ten epochs. We train the network for fifty epochs. For training on CIFAR10 [10], we use the standard VGG11 [25] network. The convolutional layers use 3×3 kernels with padding of one. We start with a learning rate of 0.1 which is decreased by a factor of 0.2 after 60, 120 and 160 epochs. We train the network for 200 epochs. We use SGD with momentum (0.9) and weight de-

cay (5×10^{-4}) for all our training. We use mean subtraction of 0.5 as a pre-processing step.

Layer	MNIST	CIFAR10
Conv+ReLU	32 filters (3x3)	64 filters (3x3)
Conv+ReLU	32 filters (3x3)	128 filters (3x3)
MaxPool	2x2	2x2
Conv+ReLU	64 filters (3x3)	256 filters (3x3)
Conv+ReLU	64 filters (3x3)	256 filters (3x3)
MaxPool	2x2	2x2
Conv+ReLU	-	512 filters (3x3)
Conv+ReLU	-	512 filters (3x3)
MaxPool	-	2x2
Conv+ReLU	-	512 filters (3x3)
Conv+ReLU	-	512 filters (3x3)
MaxPool	-	2x2
FC+ReLU	200 units	512 units
FC+ReLU	200 units	512 units
Softmax	10 units	10 units

Table 1. Overview of network architectures for MNIST [13] and CIFAR10 [10] datasets.

We compare and evaluate the following defense methods against adversarial attacks:

- **SM** - The baseline model trained using the typical Softmax loss function.
- **LS (Label Smoothing)** - The model trained using the Softmax Loss with soft labels $\{\frac{1}{90}, 0.9\}$ [27] instead of discrete labels $\{0, 1\}$
- **BReLU (Bounded ReLU)** - The model trained using bounded ReLU [29] activation function instead of ReLU. The activations are clipped between $[0, 1]$.
- **CL (CenterLoss)** - The model trained using Center-Loss [28] discussed in Section 4.1. The hyper-parameter λ was set to 1.0.
- **L2SM (L_2 -Softmax)** - The model trained using L_2 -Softmax Loss [22] as discussed in Section 4.2.
- **PCN (Power Convolutional Network)** - The model trained with power convolution modules instead of traditional convolutional and fully-connected layers, as discussed in Section 5.
- **PCN+LS (Power Convolutional Network with Label Smoothing)** - A PCN trained using soft labels $\{\frac{1}{90}, 0.9\}$

6.1. White-Box Attacks

In a white-box attack, the attacker has full access to the network to be attacked. For each of the defense methods, we generate FGSM [6] and DeepFool [18] attack for MNIST [13] and CIFAR10 [10] testset.

Table 2 provides the classification accuracy of various defense methods on adversarial examples crafted using FGSM [6] for MNIST [13] testset. We perform evaluations for four different ϵ values $\{0.1, 0.2, 0.3, 0.4\}$. Higher value of ϵ leads to larger perturbation, thus decreasing the accuracy.

Note that $\epsilon = 0$ correspond to the clean test samples without any adversarial perturbation. From the table, we find that both *PCN* and *PCN+LS* are highly robust to FGSM attack, with minimal degradation in accuracy. Specifically, for $\epsilon = 0.3$, *PCN* achieves an accuracy of 81.38% which is more than $2 \times$ factor improvement over the baseline model with accuracy 31.76%. Label Smoothing along with PCN (*PCN+LS*) further enhances the robustness to achieve an accuracy of 89.73%. The models *CL* and *L2SM* show significant improvement over the baseline, which establishes the robustness of these loss functions. A similar trend is observed with FGSM [6] attack on CIFAR10 [10] testset. Since CIFAR10 is a harder dataset, we use the ϵ values of $\{\frac{2}{255}, \frac{4}{255}, \frac{8}{255}, \frac{16}{255}\}$ to craft the FGSM attack. The classification accuracies of different methods are reported in Table 3. For $\epsilon = \frac{8}{255}$, we observe $5 \times$ improvement using *PCN* and *PCN+LS*, compared to the baseline model.

Method	$\epsilon=0$	$\epsilon=0.1$	$\epsilon=0.2$	$\epsilon=0.3$	$\epsilon=0.4$
SM	99.50	92.61	63.71	31.76	19.39
LS	99.53	95.62	85.13	44.25	15.57
BReLU	99.54	95.29	74.83	42.51	19.41
CL	99.59	96.87	88.34	59.68	23.55
L2SM	99.48	94.51	79.68	60.32	45.16
PCN	99.50	96.99	91.64	81.38	60.65
PCN+LS	99.43	97.26	93.68	89.73	75.95

Table 2. Accuracy (%) on MNIST [13] for FGSM [6] attack (with different ϵ). The best and second-best accuracies are represented in bold.

Method	$\epsilon=0$	$\epsilon=2$	$\epsilon=4$	$\epsilon=8$	$\epsilon=16$
SM	91.14	60.82	34.62	14.30	8.57
LS	91.03	66.7	58.4	54.07	51.05
BReLU	90.87	61.49	35.02	18.01	13.73
CL	91.38	64.54	49.85	41.17	35.29
L2SM	91.37	70.58	65.39	63.71	62.59
PCN	90.54	73.72	71.47	69.65	66.23
PCN+LS	90.51	80.93	79.2	76.8	71.38

Table 3. Accuracy (%) on CIFAR10 [10] for FGSM [6] attack (with different ϵ out of 255). The best and second-best accuracies are shown in bold.

Tables 4 and 5 provide the classification accuracies of different defense methods against DeepFool [18] attack, on MNIST and CIFAR10 respectively. Since, DeepFool is an iterative attack, it will mostly find a perturbation to fool the network. To evaluate using DeepFool, the iterations are carried out until the adversarial perturbation (η) causes the network to mis-classify, or the ratio of L_2 -norm of the perturbation (η) and the input (x) reaches the *max-residue-ratio* (d), as given in equation 24.

$$\frac{\|\eta\|_2}{\|x\|_2} \leq d \quad (24)$$

The evaluations are carried out with different values of $d = \{0.1, 0.2, 0.3, 0.4, 0.5\}$. From Table 4, we find that *LS* and *PCN* perform comparably against DeepFool attack on MNIST. The model *PCN+LS* achieves the best performance since it leverages the qualities of both *LS* and *PCN* models. On CIFAR10 dataset, *PCN* performs better than *LS* against DeepFool attack (see Table 5). The effect of label smoothing is less for CIFAR10, since the probability scores are lower owing to the toughness of the dataset. The models *PCN* and *PCN+LS* significantly outperform other defense methods against DeepFool attack.

Method	$d=0.1$	$d=0.2$	$d=0.3$	$d=0.4$	$d=0.5$
SM	93.24	63.22	18.73	1.89	0.53
LS	96.85	92.2	88.12	82.05	70.08
BReLU	96.15	84.33	70.13	57.25	45.5
CL	97.11	90.98	77.45	52.46	26.66
L2SM	96.5	88.22	75.94	59.47	40.31
PCN	97.06	92.18	83.46	69.25	48.54
PCN+LS	97.76	95.42	92.43	88.65	84.01

Table 4. Accuracy (%) for DeepFool [18] attack (with different max-residue-ratio d) on MNIST [13] testset. The best and second-best accuracies are represented in bold.

Method	$d=0.1$	$d=0.2$	$d=0.3$	$d=0.4$	$d=0.5$
SM	5.73	5.72	5.72	5.72	5.72
LS	57.33	43.93	31.77	21.89	14.6
BReLU	22.44	15.49	10.48	7.29	6.37
CL	51.48	29.61	14.24	8.27	6.12
L2SM	66.63	56.93	47.89	38.52	28.85
PCN	73.17	71.78	70.24	68.13	64.02
PCN+LS	80.8	79.38	78.08	76.43	74.22

Table 5. Accuracy (%) for DeepFool [18] attack (with different max-residue-ratio d) on CIFAR10 [10] testset. The best and second-best accuracies are represented in bold.

We also provide a quantitative measure of model’s robustness against DeepFool [18] attack in Table 6. The robustness measure $\rho_{adv}(\hat{k})$ for a classifier \hat{k} is computed using 25.

$$\rho_{adv}(\hat{k}) = \mathbb{E}_{\mathbf{x}} \frac{\|\mathbf{r}_{\mathbf{x}, \hat{k}}\|_2}{\|\mathbf{x}\|_2}, \quad (25)$$

where $\mathbf{r}_{\mathbf{x}, \hat{k}}$ is the generated perturbation, \mathbf{x} is the input image, and $\mathbb{E}_{\mathbf{x}}$ is the expectation over the entire test data. Similar to the classification accuracy, the robustness of *LS* is higher than *PCN* for MNIST but lower for CIFAR10. *PCN+LS* is the most robust model for both the datasets.

6.1.1 Adversarial Training

Goodfellow et al. [6] proposed to train the network simultaneously with original and crafted adversarial images to improve its stability. We analyze the effect of adversarial

Method	Robustness	Method	Robustness
SM	0.225	SM	0.014
LS	0.571	LS	0.185
BReLU	0.493	BReLU	0.057
CL	0.403	CL	0.117
L2SM	0.441	L2SM	0.285
PCN	0.479	PCN	0.549
PCN+LS	0.827	PCN+LS	0.625

Table 6. Robustness of defense methods against DeepFool [18] attack for MNIST [13] (left) and CIFAR10 [10] (right)

training on different defense models. We train the models on real and adversarial images crafted from FGSM attack with $\epsilon = 0.3$ for MNIST, and $\epsilon = \frac{8}{255}$ for CIFAR10 dataset. The classification accuracies of adversarially trained models are reported in Tables 7 and 8 for MNIST and CIFAR10 respectively. The results show that adversarial training improves the robustness for all the models. The performance of the models on MNIST dataset are comparable to each other with accuracy values above 95%. CIFAR10 results show better distinct between performance of various models. Most of the the models perform well for the ϵ value with which they were trained, but the performance degrades on other ϵ values. The models *PCN* and *PCN+LS* are consistently stable across all the ϵ values.

Method	$\epsilon=0$	$\epsilon=0.1$	$\epsilon=0.2$	$\epsilon=0.3$	$\epsilon=0.4$
SM	99.49	96.51	98.67	99.15	96.06
LS	99.45	98.4	98.77	99.31	98.79
BReLU	99.43	96.79	98.93	99.42	97.12
CL	99.45	98.37	98.41	99.36	63.61
L2SM	99.47	96.88	98.7	99.32	84.03
PCN	99.44	98.18	98.71	99.09	96.9
PCN+LS	99.48	98.65	98.8	98.93	94.13

Table 7. Accuracy (%) with adversarial training against FGSM [6] attack on MNIST [13] testset. The best and second-best accuracies are represented in bold.

Method	$\epsilon=0$	$\epsilon=2$	$\epsilon=4$	$\epsilon=8$	$\epsilon=16$
SM	83.8	71.56	67.18	71.46	43.09
LS	83.28	77.68	69.07	52.13	34.04
BReLU	85.37	72.93	67.08	80.73	31.01
CL	83.04	78.4	69.23	51.44	31.18
L2SM	84.8	73.08	68.31	74.95	49.64
PCN	87.08	73.27	75.8	76.78	61.97
PCN+LS	87.17	76.68	77.53	77.66	70.17

Table 8. Accuracy (%) with adversarial training against FGSM [6] attack on CIFAR10 [10] testset. The best and second-best accuracies are shown in bold.

6.2 Black-Box Attacks

In a typical black-box attack, the attacker has no information about the network architecture, its parameters or the training dataset. The attacker can query the network and

Attack tested on	Attack crafted on						
	SM	LS	BReLU	CL	L2SM	PCN	PCN+LS
SM	31.76*	61.41	54.22	77.15	77.88	91.22	93.84
LS	49.48	44.25*	53.63	75.44	80.47	91.76	94.69
BReLU	52.62	66.43	42.51*	80.4	79.69	90.82	93.77
CL	56.1	62.37	59.02	59.68*	79.39	90.63	94.34
L2SM	52.01	64.93	58.91	75.97	60.32*	90.65	93.59
PCN	64.15	75.7	66.55	82.37	82.7	81.38*	93.53
PCN+LS	70.18	80.83	71.49	84.95	85.29	90.49	89.73*

Table 9. Accuracy (%) on MNIST [13] against transfer attacks crafted using FGSM ($\epsilon = 0.3$). * indicates that the adversarial attacks were crafted and tested on the same network, causing maximum impact.

Attack tested on	Attack crafted on						
	SM	LS	BReLU	CL	L2SM	PCN	PCN+LS
SM	14.30*	59.14	33.63	49.62	67.13	77.77	82.91
LS	31.16	54.07*	33.28	49.86	67.26	77.84	83.11
BReLU	33.63	59.65	18.01*	50.88	67.96	77.85	82.95
CL	31.59	56.69	34.03	41.17*	67.25	77.96	83.51
L2SM	32.59	59.95	35.01	50.25	63.71*	77.76	82.78
PCN	41.33	63.6	42.37	54.81	69.63	69.65*	80.53
PCN+LS	41.48	63.48	42.29	55.5	69.98	73.74	76.8*

Table 10. Accuracy (%) on CIFAR10 [10] against transfer attacks crafted using FGSM ($\epsilon = \frac{8}{255}$). * indicates that the adversarial attacks were crafted and tested on the same network, causing maximum impact.

can get the output class label for a given input. We use the black-box attack proposed by Papernot et al. [19] to evaluate the defense models. We treat our defense models as oracle, and train substitute models using LeNet [12] architecture as described in [19]. Table 11 reports the accuracy of the defense models against FGSM attack generated using the corresponding substitute models. We observe that *PCN+LS* and *CL* models are most robust to practical black-box attacks. *PCN* comparable to *CL* and is consistent across different ϵ values.

Method	$\epsilon = 0.1$	$\epsilon = 0.2$	$\epsilon = 0.3$	$\epsilon = 0.4$
SM	98.49	87.44	55.41	32.84
LS	98.89	91.12	52.53	29.28
BReLU	98.90	91.96	66.45	39.44
CL	99.34	96.92	80.99	38.37
L2SM	98.99	93.37	56.67	26.63
PCN	99.15	96.76	77.27	28.19
PCN+LS	99.24	97.33	84.14	32.94

Table 11. Accuracy (%) against practical black-box FGSM attack (with different ϵ) on MNIST [13] testset. The best and second-best accuracies are represented in bold.

6.2.1 Transferability of Adversarial Samples

It has been shown in [19] that adversarial examples generated on one type of network can be used to fool a different type of network. This makes it easier for the attackers to generate adversarial samples using their independently trained models. Our defense model should be immune to

the attacks generated by itself, as well to the attacks generated from a different network.

Tables 9 and 10 report the accuracies on transferred attacks between different defense models. We find that the networks are more vulnerable to the transferred attacks generated using the baseline model *SM*. Among all the models, *PCN* and *PCN+LS* are most robust to transferred attacks. Also, the attacks generated using these models are less likely to fool other models. This shows that *PCN* and *PCN+LS* provide a two-way defense. Firstly, these models would be less vulnerable to any unknown adversarial attacks. Secondly, the attacks generated using these models would be less harmful for any unknown network.

7. Conclusion

In this paper, we show that feature *centrality* and *compactness* can improve a network’s robustness against adversarial attacks. CenterLoss, that follows *centrality*, and L_2 -Softmax Loss, that follows both *centrality* and *compactness*, provide better robustness compared to naive softmax loss. These properties are applied to each layer of the network using power convolutional modules, which significantly reduces the network’s vulnerability to adversarial perturbations. Label smoothing provides an additional robustness to the network. In future, we would further analyze the necessary properties for a network to be robust, and build sophisticated architectures that are provably robust to adversarial attacks.

8. ACKNOWLEDGMENTS

This research is based upon work supported by the Office of the Director of National Intelligence (ODNI), Intelligence Advanced Research Projects Activity (IARPA), via IARPA R&D Contract No. 2014-14071600012. The views and conclusions contained herein are those of the authors and should not be interpreted as necessarily representing the official policies or endorsements, either expressed or implied, of the ODNI, IARPA, or the U.S. Government. The U.S. Government is authorized to reproduce and distribute reprints for Governmental purposes notwithstanding any copyright annotation thereon.

References

- [1] N. Carlini and D. Wagner. Adversarial examples are not easily detected: Bypassing ten detection methods. *arXiv preprint arXiv:1705.07263*, 2017. [2](#)
- [2] N. Carlini and D. Wagner. Towards evaluating the robustness of neural networks. In *Security and Privacy (SP), 2017 IEEE Symposium on*, pages 39–57. IEEE, 2017. [2](#)
- [3] M. Cisse, P. Bojanowski, E. Grave, Y. Dauphin, and N. Usunier. Parseval networks: Improving robustness to adversarial examples. In *International Conference on Machine Learning*, pages 854–863, 2017. [2](#)
- [4] G. K. Dziugaite, Z. Ghahramani, and D. M. Roy. A study of the effect of jpg compression on adversarial images. *arXiv preprint arXiv:1608.00853*, 2016. [2](#)
- [5] R. Feinman, R. R. Curtin, S. Shintre, and A. B. Gardner. Detecting adversarial samples from artifacts. *arXiv preprint arXiv:1703.00410*, 2017. [2](#)
- [6] I. J. Goodfellow, J. Shlens, and C. Szegedy. Explaining and harnessing adversarial examples. *arXiv preprint arXiv:1412.6572*, 2014. [1, 2, 5, 6, 7](#)
- [7] K. Grosse, P. Manoharan, N. Papernot, M. Backes, and P. McDaniel. On the (statistical) detection of adversarial examples. *arXiv preprint arXiv:1702.06280*, 2017. [2](#)
- [8] S. Gu and L. Rigazio. Towards deep neural network architectures robust to adversarial examples. *arXiv preprint arXiv:1412.5068*, 2014. [2](#)
- [9] C. Guo, M. Rana, M. Cisse, and L. van der Maaten. Countering adversarial images using input transformations. *arXiv preprint arXiv:1711.00117*, 2017. [2](#)
- [10] A. Krizhevsky and G. Hinton. Learning multiple layers of features from tiny images. 2009. [1, 5, 6, 7, 8](#)
- [11] A. Kurakin, I. Goodfellow, and S. Bengio. Adversarial machine learning at scale. *arXiv preprint arXiv:1611.01236*, 2016. [2](#)
- [12] Y. LeCun, L. Bottou, Y. Bengio, and P. Haffner. Gradient-based learning applied to document recognition. *Proceedings of the IEEE*, 86(11):2278–2324, 1998. [8](#)
- [13] Y. LeCun, C. Cortes, and C. J. Burges. MNIST handwritten digit database. *AT&T Labs [Online]. Available: http://yann.lecun.com/exdb/mnist*, 2, 2010. [4, 5, 6, 7, 8](#)
- [14] J. Lu, T. Issaranon, and D. Forsyth. Safetynet: Detecting and rejecting adversarial examples robustly. *arXiv preprint arXiv:1704.00103*, 2017. [2](#)
- [15] J. H. Metzen, T. Genewein, V. Fischer, and B. Bischoff. On detecting adversarial perturbations. *arXiv preprint arXiv:1702.04267*, 2017. [2](#)
- [16] T. Miyato, S.-i. Maeda, M. Koyama, and S. Ishii. Virtual adversarial training: a regularization method for supervised and semi-supervised learning. *arXiv preprint arXiv:1704.03976*, 2017. [2](#)
- [17] S.-M. Moosavi-Dezfooli, A. Fawzi, O. Fawzi, and P. Frossard. Universal adversarial perturbations. *arXiv preprint arXiv:1610.08401*, 2016. [1, 2](#)
- [18] S.-M. Moosavi-Dezfooli, A. Fawzi, and P. Frossard. Deepfool: a simple and accurate method to fool deep neural networks. In *Proceedings of the IEEE Conference on Computer Vision and Pattern Recognition*, pages 2574–2582, 2016. [1, 2, 5, 6, 7](#)
- [19] N. Papernot, P. McDaniel, I. Goodfellow, S. Jha, Z. B. Celik, and A. Swami. Practical black-box attacks against machine learning. In *Proceedings of the 2017 ACM on Asia Conference on Computer and Communications Security*, pages 506–519. ACM, 2017. [8](#)
- [20] N. Papernot, P. McDaniel, S. Jha, M. Fredrikson, Z. B. Celik, and A. Swami. The limitations of deep learning in adversarial settings. In *Security and Privacy (EuroS&P), 2016 IEEE European Symposium on*, pages 372–387. IEEE, 2016. [2](#)
- [21] N. Papernot, P. McDaniel, X. Wu, S. Jha, and A. Swami. Distillation as a defense to adversarial perturbations against deep neural networks. In *Security and Privacy (SP), 2016 IEEE Symposium on*, pages 582–597. IEEE, 2016. [2, 5](#)
- [22] R. Ranjan, C. D. Castillo, and R. Chellappa. L2-constrained softmax loss for discriminative face verification. *arXiv preprint arXiv:1703.09507*, 2017. [2, 3, 4, 6](#)
- [23] J. Rauber, W. Brendel, and M. Bethge. Foolbox v0. 8.0: A python toolbox to benchmark the robustness of machine learning models. *arXiv preprint arXiv:1707.04131*, 2017. [5](#)
- [24] U. Shaham, Y. Yamada, and S. Negahban. Understanding adversarial training: Increasing local stability of neural nets through robust optimization. *arXiv preprint arXiv:1511.05432*, 2015. [2](#)
- [25] K. Simonyan and A. Zisserman. Very deep convolutional networks for large-scale image recognition. *arXiv preprint arXiv:1409.1556*, 2014. [5](#)
- [26] C. Szegedy, W. Zaremba, I. Sutskever, J. Bruna, D. Erhan, I. Goodfellow, and R. Fergus. Intriguing properties of neural networks. *arXiv preprint arXiv:1312.6199*, 2013. [1, 2](#)
- [27] D. Warde-Farley and I. Goodfellow. Adversarial perturbations of deep neural networks. *Perturbations, Optimization, and Statistics*, page 311, 2016. [2, 6](#)
- [28] Y. Wen, K. Zhang, Z. Li, and Y. Qiao. A discriminative feature learning approach for deep face recognition. In *European Conference on Computer Vision*, pages 499–515. Springer, 2016. [2, 3, 6](#)
- [29] V. Zantedeschi, M.-I. Nicolae, and A. Rawat. Efficient defenses against adversarial attacks. *arXiv preprint arXiv:1707.06728*, 2017. [2, 6](#)